J. KSIAM Vol.19, No.2, 197–215, 2015 http://dx.doi.org/10.12941/jksiam.2015.19.197

CONSEQUENCE OF BACKWARD EULER AND CRANK–NICOLSOM TECHNIQUES IN THE FINITE ELEMENT MODEL FOR THE NUMERICAL SOLUTION OF VARIABLY SATURATED FLOW PROBLEMS

M.S. ISLAM

DEPARTMENT OF MATHEMATICS, SHAHJALAL UNIVERSITY OF SCIENCE & TECHNOLOGY, SYLHET-3114, BANGLADESH

E-mail address: sislam_25@yahoo.com

ABSTRACT. Modeling water flow in variably saturated, porous media is important in many branches of science and engineering. Highly nonlinear relationships between water content and hydraulic conductivity and soil-water pressure result in very steep wetting fronts causing numerical problems. These include poor efficiency when modeling water infiltration into very dry porous media, and numerical oscillation near a steep wetting front. A one-dimensional finite element formulation is developed for the numerical simulation of variably saturated flow systems. First order backward Euler implicit and second order Crank–Nicolson time discretization schemes are adopted as a solution strategy in this formulation based on Picard and Newton iterative techniques. Five examples are used to investigate the numerical performance of two approaches and the different factors are highlighted that can affect their convergence and efficiency. The first test case deals with sharp moisture front that infiltrates into the soil column. It shows the capability of providing a mass-conservative behavior. Saturated conditions are not developed in the second test case. Involving of dry initial condition and steep wetting front are the main numerical complexity of the third test example. Fourth test case is a rapid infiltration of water from the surface, followed by a period of redistribution of the water due to the dynamic boundary condition. The last one-dimensional test case involves flow into a layered soil with variable initial conditions. The numerical results indicate that the Crank–Nicolson scheme is inefficient compared to fully implicit backward Euler scheme for the layered soil problem but offers same accuracy for the other homogeneous soil cases.

1. INTRODUCTION

The accurate numerical simulation of water flow through soils is an important environmental problem and has applications in various fields including industrial, hydrological and agricultural engineering, waste and water management, ground water engineering, chemical contaminants tracing, and rainfall–runoff modeling. For some cases, soil profiles can be considered homogenous but in most cases, soil profiles are heterogeneous and can consist of distinct soil

Received by the editors March 15 2015; Revised May 21 2015; Accepted in revised form May 26 2015; Published online June 13 2015.

Key words and phrases. Richards' equation; Backward Euler, Implicit, Crank–Nicolson, Numerical solution, Variably saturated flow.

layers. Vertical water flow through a one dimensional variably saturated soil profile is described by Richards' equation and it can be written in the following form:

$$S(\psi)\frac{\partial \psi}{\partial t} = \frac{\partial}{\partial z}\left(K(\psi)\left(\frac{\partial \psi}{\partial z} + 1\right)\right) \tag{1.1}$$

where, ψ is the pressure head $[L]$, t is time $[T]$, z denotes the vertical distance from the soil surface downward $[L]$, $K(\psi$ is the hydraulic conductivity $[LT^{-1}]$ $(K(\psi) = K_r(\psi)K_s$, K_r and K_s are the relative and saturated hydraulic conductivity respectively), $S(\psi) = \frac{d\theta}{d\psi} + \left(\frac{\theta}{\phi}\right) S_s$ is the general storage term, θ is the volumetric water content, $\psi \frac{d\theta}{d\psi}$ is the specific soil moisture capacity $[L^{-1}]$, ϕ is porosity, S_s is specific storage.

Mathematical modeling of fluid flow usually results in systems of highly nonlinear partial differential equations which are not solvable analytically unless unrealistic and oversimplifying assumptions are made regarding the attributes, dynamics, and properties of the physical systems. A variety of numerical models have been proposed on the basis of the finite difference, finite element, and finite volume methods to simulate flow problems. In particular, a hybrid numerical scheme based on the Euler implicit method, quasi linearization and uniform Haar wavelets has been developed for the numerical solutions of highly nonlinear partial differential equation with Dirichlet's boundary conditions [1], forward finite difference, quasi-linearisation process and polynomial differential quadrature method with Dirichlet and Neumann boundary condition [2, 3], Crank–Nicolson finite difference scheme and Haar wavelets for various types of hyperbolic telegraph equations [4], finite element technique for two point boundary value problem [5, 6], B-spline differential quadrature method for two-dimensional sine-Gordon equation with Neumann boundary condition [7].

Low order finite difference method or finite element method [8, 9, 10, 11, 12], mixed-hybrid finite element [13] and discontinuous Galerkin finite element [14] schemes are usually perform to spatial discretization of equation (1.1). The simplest numerical technique for solving the nonlinear Richards' equation is explicit two-level time discretization approach. This approach give up a linear system of equations, minimizes storage requisites and on a per time step basis it represents a least cost opportunity. However, stability constraints for explicit methods are relatively severe, and therefore for long simulations or for problems which involve fine spatial resolution, the small time step sizes essential to keep a stable solution can provide these schemes very costly on a per simulation basis. Usually, implicit time discretizations scheme is unconditionally stable for solving Richards' equation numerically. The weighted two-level implicit discretization most commonly used results in a nonlinear system of equations, and the conventional approach has been to solve this nonlinear system using an iterative procedure.

Newton and Picard methods are two commonly iterative techniques with the simpler Picard method being the more popular of the two [15, 16, 17, 18, 19, 20, 21] . In certain situations where the relative permeability and water saturation functions are highly nonlinear, convergence difficulties may be encountered in solving the flow equation by using the Picard iterative method. To overcome this problem, the Newton–Raphson method should be considered. The

Newton procedure has been extensively used in conjunction with finite difference techniques to solve variably saturated flow problems.

In this study, backward Euler scheme is used as a one of the most popular time approximation for the Richards' equation. The nonlinear dependency of moisture content on pressure head, the Richards' equation become highly nonlinear, as a result iterative calculation and linearization are needed. From a practical viewpoint, the Picard method is used in this study because it is simple and exhibits a good performance in many problems [22, 23]. Although, there are several successful iterative schemes have been proposed [23, 24, 25, 26].

Picard iterative scheme converge linearly, computationally cheap on a per-iteration basis, and preserves symmetry of the discrete system of equations, accordingly this technique has received very much concentration. However, under certain circumstances, a number of studied has been proved that this scheme may diverge [8, 18] and verified theoretically [27]. Nonsymmetric system matrices attains in the Newton scheme which is more complex and expensive, however it achieves a higher rate of convergence and more robust for certain types of problems than Picard linearization. But use of the Newton scheme has been limited to one- and two-dimensional unsaturated flow models [15, 18, 28, 29].

2. Numerical Procedures

2.1. **Finite element models.** For solving Richards' equation (1.1), the finite element Galerkin discretization in space and first order backward Euler and second order Crank–Nicolson finite difference time approximation schemes are used in this study.

The spatial domain is sibdivided into *M-1* elements in the finite element network. Let the pressure head function ψ be approximated by a trial function of the form

$$\psi\left(z,t\right) \approx \hat{\psi}\left(z,t\right) = \sum_{J=1}^{M} N_J\left(z\right)\psi_J(t) \tag{2.1}$$

where $N_J\left(z\right)$ and $\psi_J(t)$ are nodal basis shape functions and nodal values of ψ at time t, respectively, M is the total number of nodes in the finite element model. In local coordinate space $-1 \leq \xi \leq 1$, the approximating function for each element (e) is $\hat{\psi}^{(e)} = \sum_{i=1}^{2} N_i^{(e)}\left(\xi\right)\psi_i^{(e)}\left(t\right) = \frac{1}{2}\left(1-\xi\right)\psi_1^{(e)}\left(t\right) + \frac{1}{2}\left(1+\xi\right)\psi_2^{(e)}\left(t\right)$ which we can write in vector form as $\hat{\psi}^{(e)} = \left(\mathbf{N}^{(e)}\left(\xi\right)\right)^T \mathbf{\Psi}^{(e)}(t)$. The global function (2.1) becomes

$$\hat{\psi} = \sum_{e=1}^{M-1}\left(\mathbf{N}^{(e)}\right)^T\mathbf{\Psi}^{(e)} = \sum_{e=1}^{M-1}\hat{\psi}^{(e)} \tag{2.2}$$

The symmetric weak formulation of Galerkin's method applied to (1.1) yields the system of ordinary differential equations [30]

$$\mathbf{A}\left(\mathbf{\Psi}\right)\mathbf{\Psi} + \mathbf{F}\left(\mathbf{\Psi}\right)\frac{\mathrm{d}\mathbf{\Psi}}{\mathrm{dt}} = \mathbf{q}\left(\mathrm{t}\right) - \mathbf{b}(\mathbf{\Psi}) \tag{2.3}$$

where $\mathbf{\Psi}$ is the vector of undetermined coefficients corresponding to the values of pressure head at each node, *q* contains the specified Darcy flux boundary conditions, and *A*, *b*, and *F* are

given over local subdomain element $\mathbf{\Omega}^{(e)}$ as

$$\mathbf{A}^{(e)} = \int_{\mathbf{\Omega}^{(e)}} \mathbf{K}_s^{(e)} K_r(\hat{\psi}^{(e)}) \frac{\mathbf{dN^{(e)}}}{\mathbf{dz}} \left(\frac{\mathbf{dN^{(e)}}}{\mathbf{dz}} \right)^T dz \tag{2.4}$$

$$\mathbf{b}^{(e)} = \int_{\mathbf{\Omega}^{(e)}} \mathbf{K}_s^{(e)} K_r(\hat{\psi}^{(e)}) \frac{\mathbf{dN^{(e)}}}{\mathbf{dz}} dz \tag{2.5}$$

$$\mathbf{F}^{(e)} = \int_{\mathbf{\Omega}^{(e)}} S(\hat{\psi}^{(e)}) \mathbf{N}^{(e)} (\mathbf{N}^{(e)})^T dz \tag{2.6}$$

Here $\mathbf{N}^T$ to denote the transpose of $\mathbf{N}$.

The nonlinear integrals in (2.4), (2.5), and (2.6) are evaluated by the second order Gaussian quadrature formula introducing an additional source of numerical error. The magnitude of this error will depend on the degree of nonlinearity in the $K_r(\psi)$ and $S(\psi)$ characteristic equations and can be minimized by using higher order numerical quadrature or a smaller mesh size Δz.

2.2. **Time differencing.** The time derivative term in (2.3) is approximated by a λ-weighted finite difference technique. We obtain

$$\mathbf{A}\left(\mathbf{\Psi}^{k+\lambda}\right)\mathbf{\Psi}^{k+\lambda} + \mathbf{F}\left(\mathbf{\Psi}^{k+\lambda}\right)\frac{\mathbf{\Psi}^{k+1} - \mathbf{\Psi}^{k}}{\Delta t} = \mathbf{q}\left(t^{k+\lambda}\right) - \mathbf{b}(\mathbf{\Psi}^{k+\lambda}) \tag{2.7}$$

$$\text{where} \mathbf{\Psi}^{k+\lambda} = \lambda \mathbf{\Psi}^{k+1} + (1-\lambda)\mathbf{\Psi}^{k}; 0 \leq \lambda \leq 1 \tag{2.8}$$

and k denotes the time step iteration.

The equations (2.7) is a system of nonlinear in $\mathbf{\Psi}^{k+1}$ and $\lambda = 0.5$ and $\lambda = 1$ are correspond the Crank–Nicolson and backward Euler implicit scheme respectively.

3. ITERATIVE METHODS

The governing equation for variably saturated flow requires soil hydraulic functions that describe the relationship between soil water pressure and hydraulic conductivity as a function of soil moisture content. Generally, these functions are highly nonlinear and their use substantially increases computational complexity. Especially, the derivatives of moisture content can exhibit sharp changes near the saturation. It is this nonlinear dependency of the moisture content on the pressure head that makes the numerical solution of Richards' equation problematic and requires sophisticated numerical methods in order to overcome convergence problems and/or poor computational efficiency. Since the system of the equation is nonlinear, iterative calculation and linearization are needed. In linearization schemes such as the Picard and the Newton, the number of iterations needed to converge is a determining factor for the simulation efficiency. To this purpose, convergence rate is often enhanced by providing the solver with an initial estimate that is closer to the final solution for the current time step. This can be obtained by taking the initial guess from the previous time step and by choosing a sufficiently small time step size. Thus, numerical algorithms often include an empirical time step adaptation criterion.

3.1. **Newton scheme.** Let us consider

$$\mathbf{f}\left(\mathbf{\Psi}^{k+1}\right)=\mathbf{A}\left(\mathbf{\Psi}^{k+\lambda}\right)\mathbf{\Psi}^{k+\lambda}+\mathbf{F}\left(\mathbf{\Psi}^{k+\lambda}\right)\frac{\mathbf{\Psi}^{k+1}-\mathbf{\Psi}^{k}}{\Delta t}-\mathbf{q}\left(t^{k+\lambda}\right)-\mathbf{b}\left(\mathbf{\Psi}^{k+\lambda}\right)=0 \tag{3.1}$$

Here m stands for iteration index, so the Newton scheme [30] is

$$\mathbf{f}'\left(\mathbf{\Psi}^{k+1,\ m}\right)\mathbf{h}=-\mathbf{f}\left(\mathbf{\Psi}^{k+1,\ m}\right) \tag{3.2}$$

$$\text{where } \mathbf{h}=\mathbf{\Psi}^{k+\lambda,\ m+1}-\mathbf{\Psi}^{k+\lambda,\ m} \tag{3.3}$$

and

$$f'_{ij}=\lambda A_{ij}+\frac{1}{\Delta t^{k+1}}F_{ij}+\sum_{s}\frac{\partial A_{is}}{\partial\psi_j^{k+1}}\psi_s^{k+\lambda}+\frac{1}{\Delta t^{k+1}}\sum_{s}\frac{\partial F_{is}}{\partial\psi_j^{k+1}}\left(\psi_s^{k+1}-\psi_s^{k}\right)+\frac{\partial b_i}{\partial\psi_j^{k+1}} \tag{3.4}$$

is the *ij*th component of the Jacobian matrix $\mathbf{f}'\left(\mathbf{\Psi}^{k+1}\right)$.

The Newton iteration scheme can be thought of as a parallel chord method with updating, that is, we use the "tangent" $\mathbf{f}'$ as the iteration matrix, and update this slope matrix at each iteration.

3.2. **Picard Scheme.** The simple formulation of Picard scheme [23] can be obtained directly from (2.7) by iterating with all linear occurrences of $\mathbf{\Psi}^{k+1}$ taken at the current iteration level $m+1$ and all nonlinear occurrences at the previous level m. We get,

$$\left[\lambda\mathbf{A}\left(\lambda\mathbf{\Psi}^{k+\lambda,\ m}\right)+\frac{1}{\Delta t}\mathbf{F}\left(\mathbf{\Psi}^{k+\lambda,\ m}\right)\right]\mathbf{h}=-\mathbf{f}\left(\mathbf{\Psi}^{k+1,\ m}\right) \tag{3.5}$$

where $\mathbf{h}=\mathbf{\Psi}^{k+\lambda,\ m+1}-\mathbf{\Psi}^{k+\lambda,\ m}$.

From (3.2) and (3.5), it is evident that the Picard scheme is an approximate Newton method. The Newton scheme is quadratically convergent, while Picard converges only linearly under suitable conditions. Newton linearization generates a nonsymmetric system matrix, but Picard preserves the symmetry of the original discretization is the important difference between these two schemes. This factor is important in evaluating the relative efficiency of the two schemes, since different storage and linear solver algorithms can be used to exploit these structural differences. Also, the calculation of the three derivative terms in the Jacobian makes the Newton scheme more costly and algebraically complex than Picard.

4. Constitutive relationships

The numerical solution to Richards' equation is based on knowledge of the relation between the pore pressure head and the water content, the water content and the unsaturated hydraulic conductivity. The most commonly used relationships are the Brooks-Corey [31] and the van Genuchten [32] model. These two models illustrated in detail as follows:

4.1. **The Brooks-Corey model.** The constitutive relationships proposed by Brooks and Corey [31] are given by;

$$\theta(\psi) = \theta_r + (\theta_s - \theta_r)\left(\frac{\psi_d}{\psi}\right) \text{ if } \psi \le \psi_d \tag{4.1}$$

$$\theta(\psi) = \theta_s \text{ if } \psi > \psi_d \tag{4.2}$$

$$K(\psi) = K_s\left[\frac{\theta(\psi) - \theta_r}{\theta_s - \theta_r}\right]^{3+2/n} \text{ if } \psi \le \psi_d \tag{4.3}$$

$$K(\psi) = K_s \text{ if } \psi > \psi_d \tag{4.4}$$

$$c(\psi) = n\frac{\theta_s - \theta_r}{|\psi_d|}\left(\frac{\psi_d}{\psi}\right)^{n+1} \text{ if } \psi \le \psi_d \tag{4.5}$$

$$c(\psi) = 0 \text{ if } \psi > \psi_d \tag{4.6}$$

where $\psi_d = -\frac{1}{\alpha}$ is air entry pressure head [L], α is mean pore size, θ_r the residual moisture content, θ_s is porosity, $c(\psi)$ is moisture capacity, K_s is saturated hydraulic conductivity and $n = 1 - \frac{1}{m}$ is a pore-size distribution index.

4.2. **The van Genuchten model.** The most commonly used empirical constitutive relations for moisture content and hydraulic conductivity is due to the work of van Genuchten [32] and are given by;

$$\theta(\psi) = \theta_r + \frac{\theta_s - \theta_r}{[1 + |\alpha\psi|^n]^m} \text{ if } \psi \le 0 \tag{4.7}$$

$$\theta(\psi) = \theta_s \text{ if } \psi > 0 \tag{4.8}$$

$$K(\psi) = K_s\left[\frac{\theta - \theta_r}{\theta_s - \theta_r}\right]^{\frac{1}{2}}\left\{1 - \left[1 - \left(\frac{\theta - \theta_r}{\theta_s - \theta_r}\right)^{\frac{1}{m}}\right]^m\right\}^2 \text{ if } \psi \le 0 \tag{4.9}$$

$$K(\psi) = K_s \text{ if } \psi > 0 \tag{4.10}$$

$$c(\psi) = \alpha m n\frac{\theta_s - \theta_r}{[1 + |\alpha\psi|^n]^{m+1}}|\alpha\psi|^{n-1} \text{ if } \psi \le 0 \tag{4.11}$$

$$c(\psi) = 0 \text{ if } \psi > 0 \tag{4.12}$$

The characteristic equations given above were used in the stated test simulations. The particular curves used for each test case are indicated, along with the corresponding parameter values. The method used to evaluate the moisture content and its derivative needed in the Jacobian of the Newton scheme, may affect the convergence behavior of the iterative schemes, due to possible discontinuities, steep gradients, and points of inflection in these curves and their derivatives. Numerical differentiation is often used to prevent floating point overflow near singularities or to avoid oscillations around points of inflection. Besides, the highly nonlinear

dependency of the hydraulic properties on the pressure head makes solution of the Richards' equation problematic, and requiring a sophisticated numerical scheme.

5. NUMERICAL RESULTS AND DISCUSSIONS

In the numerical experiments, dynamic time stepping control is used to adjust step size of time during simulation according to the convergence behavior of the nonlinear iteration scheme. A convergence tolerance is specified for each time step, along with a maximum number of iterations, *maxit.* Starting time step size is Δt_0 and simulation proceed until achieve the maximum time T_{max}. The current time step size is increased by a factor of Δt_{mag} to a maximum size of Δt_{max} if convergence is achieved in fewer than $maxit_1$ iterations, it is remain unchanged if convergence required between $maxit_1$ and $maxit_2$ iterations, and it is decreased by a factor of Δt_{red} to a minimum of Δt_{min} if convergence required more than $maxit_2$ iterations. If convergence is not achieved within *maxit*, the solution at the current time level is recomputed using a reduced time step size to the minimum time step size Δt_{min}. For the first time step of simulation, the initial conditions are used as the first solution estimate for the iterative procedure. For subsequent time steps of simulation the pressure head solution from the previous step is used as the first estimate. Thus time step size has a direct effect on convergence behavior, via its influence on the quality of the initial solution estimate. Back-stepping is also triggered if linear solver failed or if the convergence or residual errors become larger than maximum allowable convergence or residual error in the nonlinear solution. BiCGSTAB, biconjugate gradients stabilized method with the tolerance 10^{-10} is used to solve the generated system of linear equations and maximum iteration is 1000. For the nonlinear iterative methods, the infinity norm (l_∞) of the convergence error is used as the termination criterion; that is, when $\left\| \mathbf{\Psi}^{k+\lambda,\ m+1} - \mathbf{\Psi}^{k+\lambda,\ m} \right\| \leq tol$ is satisfied, convergence is achieved. The residual error ($\left\| \mathbf{f}\left(\mathbf{\Psi}^{k+1,\ m}\right) \right\|$) is computed using l_∞ and l_2 norms. For evaluating the performance of the proposed schemes, all numerical simulations were run on Dell INSPIRON, 2.56 GHz system.

5.1. **Test case 1.** This problem considers a soil column of $2m$ deep discretized with a vertical resolution $\Delta \mathrm{z} = 0.00625m$. The initial pressure head distribution is $\psi\left(z, 0\right) = z - 2$. At the bottom of the column, a water table boundary condition (i.e., $\psi\left(0, t\right) = 0$) is imposed, while a time-dependent Dirichlet condition is imposed at the top boundary

$$\psi\left(2, t\right) = \begin{cases} -0.05 + 0.03 \sin\left(\frac{2\pi t}{100000}\right) & \text{if } \ 0 < t \leq 100000 \\ \ \ 0.1 & \text{if } \ 100000 < t \leq 180000 \\ -0.05 + 2952.45 \exp\left(-t/18204.8\right) & \text{if } \ 180000 < t \leq 300000 \end{cases}$$

The soil hydraulic properties are described by the van Genuchten mode. The soil parameters are $\theta_s = 0.410$, $\theta_r = 0.095$, $\alpha = 1.9/m$, $n = 1.31$ and $K_s = 0.062\, m/day$.

The Dirichlet boundary condition leads to significant ponding between $100000s$ and $200000s$, and this type of boundary condition, prominent in coupled groundwater/surface water modeling, is a source of difficulty in the iterative schemes.

These soil properties correspond to an unconsolidated clay loam with a nonuniform grain size distribution [33]. Numerical solvers have to face difficulty in the second period of the simulation ($100000 < t \leq 180000s$). Because of sudden increase of the upper Dirichlet boundary condition to a positive value of $0.1m$ (ponding), it creates a sharp moisture front that infiltrates into the soil column. Ponding decreases exponentially the beginning of the third period ($t > 180000s$), reaching to a final value -0.05 m with asymptotically, and by the end of the simulation the entire column is close to full saturation.

The computed pressure head profiles by Picard and Newton iterative schemes for backward Euler and Crank–Nicolson techniques at times *35000s*, *155000s* and *300000s* including initial conditions are displayed in FIGURE 1. The solution profile at $t = 155000s$, which falls within the ponding period, shows the excess water that forms at the soil surface and the rather sharp moisture front that is generated. These solutions are very similar those reported in the literature [34, 35, 36, 37].

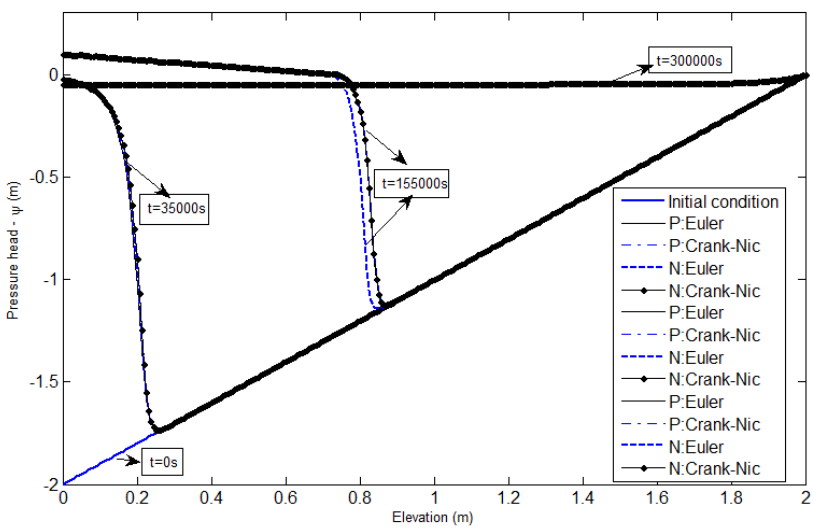

FIGURE 1. Pressure head profiles for Picard (Euler and Crank–Nicolson) and Newton (Euler and Crank–Nicolson) schemes at various times (P=Picard, N=Newton, Crank–Nic=Crank–Nicolson)

A comparison of computational statistics, such as the cumulative mass balance errors, the relative cumulative mass balance errors (%), the total number of time steps, and the nonlinear iterations per time steps for the various runs for the two time discretization approaches, are tabulated in TABLE 1. From these statistics in TABLE 1 it can be concluded that all runs have adequate and comparable accuracy. The cumulative mass balance errors almost zero for all the cases and their plots are presented in FIGURE 2.

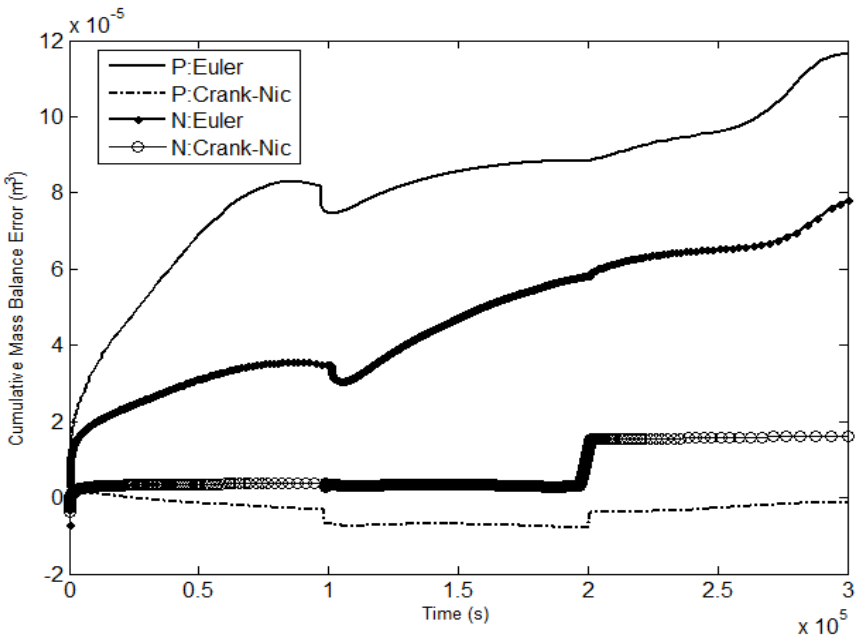

FIGURE 2. Evolution of mass balance errors for the entire simulation of Test case 1

TABLE 1. Summary statistics of the Test case 1. [*ite=iteration]

	Picard		Newton	
	Euler	Crank–Nicolson	Euler	Crank–Nicolson
MBE (m^3)	1.169e-4	-1.384e-6	7.791e-5	1.608e-5
MBE (%)	2.116e+0	-2.557e-2	1.422e+0	2.965e-1
No. of Time Steps	2033	4741	914	6298
NL ite/Time steps	5.58	5.00	6.04	4.87

5.2. **Test case 2.** Example 2 is a standard test problem that has been previously examined [38, 39, 40, 41]. The domain of this test problem is short and saturated conditions are not developed. In this test case, constant pressure head boundary conditions are imposed, at the bottom and top of the soil column are *-10m* and *-0.75m* respectively. The initial pressure head is *-10m*. A *0.3m* column of soil with van Genuchten parameters $\theta_s = 0.368$, $\theta_r = 0.102$, $\alpha = 3.35/m$, $n = 2.0$ and $K_s = 7.970\, m/day$.

The performance of the methods under these conditions is shown in TABLE 2, and pressure head profiles for 121 nodes are illustrated in FIGURE 3. As can be seen, all the evaluated methods clearly outperform the conventional algorithm and these methods seem to handle this test case without any significant problem. It is also noted that the performance of the schemes

in all cases is very similar to that of the published reports [39, 40, 41]. Acceptable cumulative mass balance errors are shown in FIGURE 4.

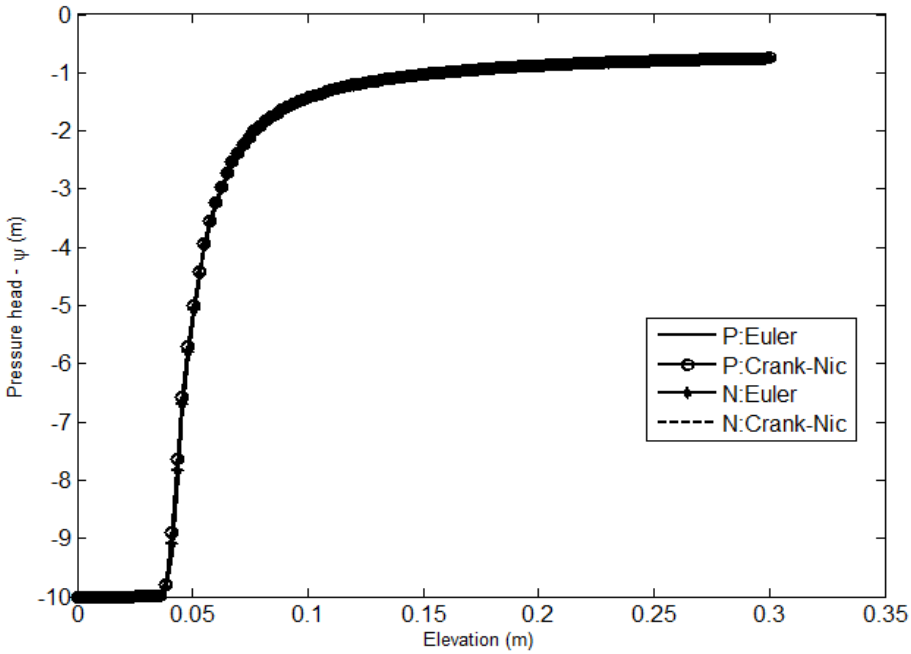

FIGURE 3. Pressure head profiles at *0.20 days* for the Picard (Euler and Crank–Nicolson) and Newton (Euler and Crank–Nicolson) iterative schemes

TABLE 2. Summary statistics of the Test case 2

	Picard		Newton	
	Euler	Crank–Nicolson	Euler	Crank–Nicolson
MBE (m^3)	1.307e-4	1.182e-4	1.298e-4	9.846e-5
MBE (%)	1.627e+1	1.540e+1	1.617e+1	1.257e+1
No. of Time Steps	1609	999	3900	2322
NL ite/Time steps	6.01	6.10	6.01	6.02

5.3. **Test Case 3.** It is a vertical infiltration problem in a *10m* soil column with $\Delta z = 0.05\,m$ and has been already analyzed in details [33, 39, 42]. It has constant head boundary conditions at both top ($\psi\,(10,t) = 0.1$) and bottom ($\psi\,(0,t) = 0.0$) boundaries and a hydrostatic equilibrium initial condition ($\psi\,(z,0) = -z$). This soil column is parameterized using the

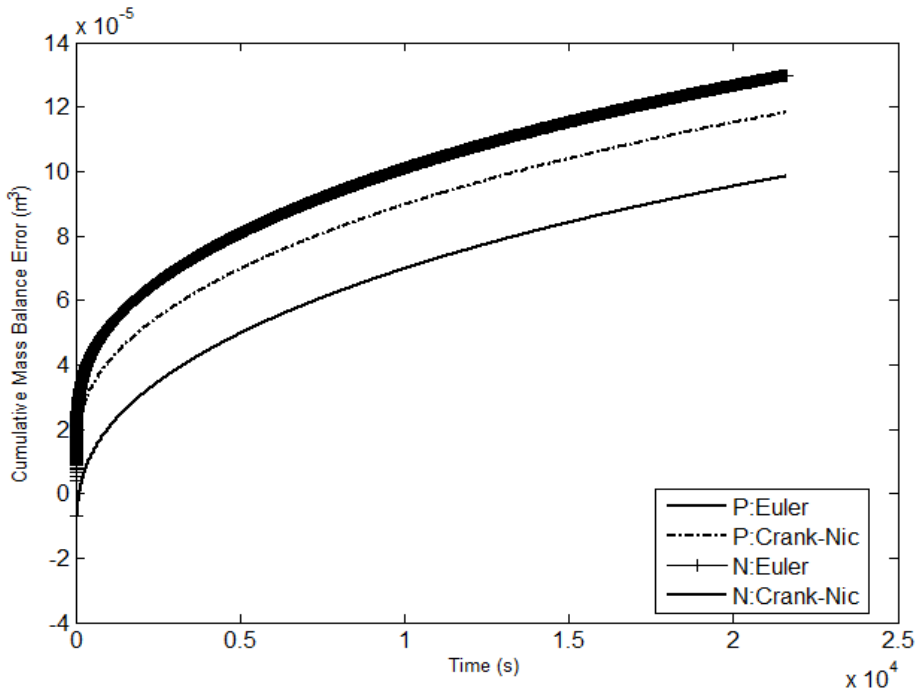

FIGURE 4. Evolution of mass balance errors for the entire simulation of Test case 2

van Genuchten relationships with $\theta_s = 0.301$, $\theta_r = 0.093$, $\alpha = 5.47/m$, $n = 4.264$ and $K_s = 5.040\, m/days$. The combination of the initial and boundary conditions along with the constitutive relationships makes it a very difficult problem, since the solution includes an extremely sharp front in space that moves through the domain as a function of time.

FIGURE 5 illustrates the simulation profiles at time t =*0.25 days* for all cases and all the solutions are very similar to the one reported in the literature [39, 40, 41] and shows excellent mass balance error which is displayed in FIGURE 6. Results are shown in TABLE 3 document that satisfied the objective of this study.

TABLE 3. Summary statistics of the Test case 3

	Picard		Newton	
	Euler	Crank–Nicolson	Euler	Crank–Nicolson
MBE (m^3)	5.346e-4	5.394e-4	5.373e-4	5.334e-4
MBE (%)	8.930e+1	8.861e+1	8.951e+1	8.906e+1
No. of Time Steps	1037	593	321	259
NL ite/Time steps	5.53	5.61	5.58	5.41

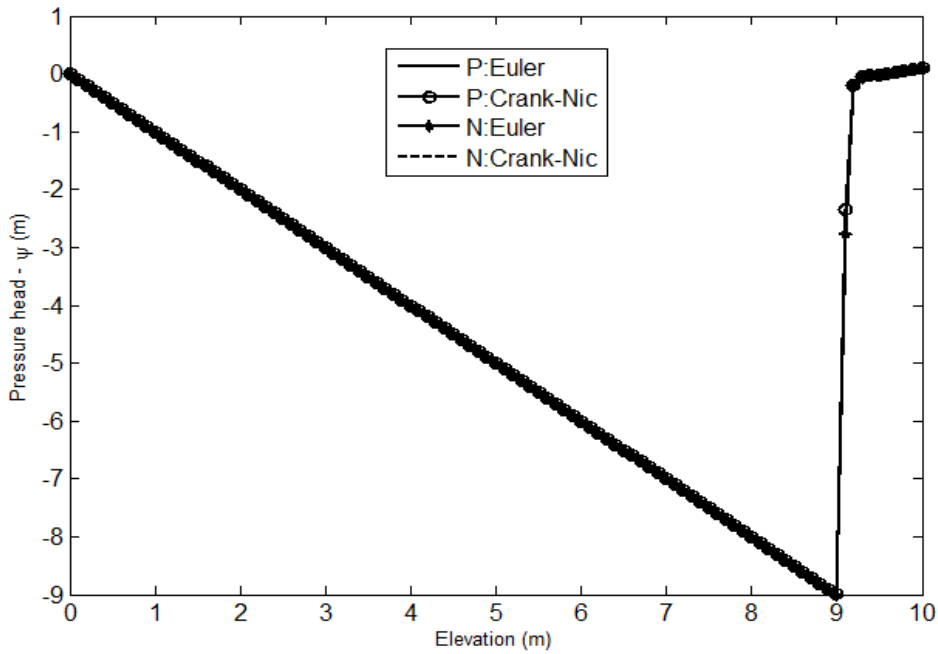

FIGURE 5. Pressure head profiles at time *0.25 days* for the Picard (Euler and Crank–Nicolson) and Newton (Euler and Crank–Nicolson) iterative schemes

5.4. **Test case 4.** Present test problem involves vertical infiltration with redistribution [42]. This problem considers a soil column of $5m$ deep discretized with a vertical resolution Δz $= 0.0125m$. It has a constant head boundary condition ($\psi\,(0,t) = 0.0$) at the bottom of the domain and a time dependent boundary condition ($\psi\,(10,t) = -10(1.0 - 1.01e^{-t})$) at the top of the domain with hydrostatic equilibrium initial conditions ($\psi\,(z,0) = -z$). The time varying boundary condition yields a difficult two-front problem. This soil column is parameterized using the van Genuchten relationships with $\theta_s = 0.301$, $\theta_r = 0.093$, $\alpha = 5.47/m$, $n = 4.264.0$ and $K_s = 5.040\,m/days$.

FIGURE 7 shows the comparison of pressure head solution profiles for all cases and similar with the previous studies [40, 43]. It is evident from these figures that there is a rapid infiltration of water from the surface, followed by a period of redistribution of the water due to the dynamic boundary condition at the top of the domain. Cumulative mass balance error plot is displayed in FIGURE 8 and computational performances are illustrated by TABLE 4. Both of them ensure the accuracy of fully implicit backward Euler and Crank–Nicolson approximations.

5.5. **Test case 5.** This case involves vertical drainage through a layered soil from initially saturated conditions. At time $t = 0$, the pressure head at the base of the column is reduced from

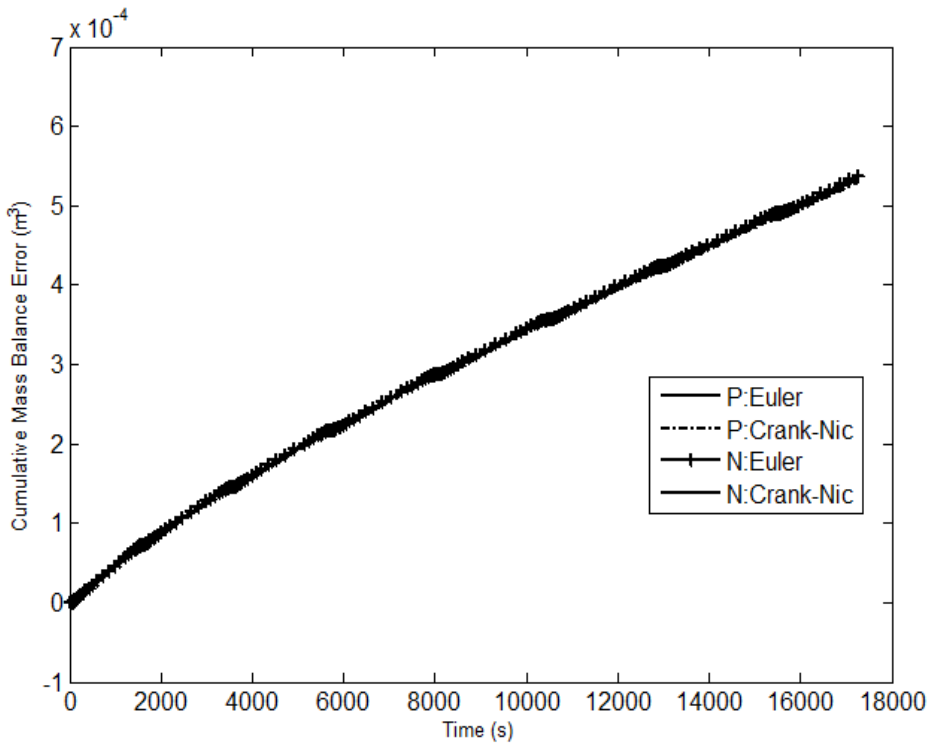

FIGURE 6. Evolution of mass balance errors for the entire simulation of Test case 3

TABLE 4. Summary statistics of the Test case 4

	Picard		Newton	
	Euler	Crank–Nicolson	Euler	Crank–Nicolson
MBE (m^3)	1.497e-2	1.519e-2	1.613e-2	1.505e-2
MBE (%)	8.082e+1	8.915e+1	8.875e+1	8.916e+1
No. of Time Steps	2672	1673	2024	1353
NL/Time steps	6.09	5.95	5.97	5.87

2 to $0m$. During the subsequent drainage, a no flow boundary condition is applied to the top of the column. This problem is considered to be a challenging test for numerical methods because a sharp discontinuity in the moisture content occurs at the interface between two material layers [36, 37, 44, 45].

The Brooks-Corey model is used to prescribe the pressure-moisture relationship. The hydraulic properties of the soils are given in TABLE 5. The soil profile is Soil-I for $0<z<0.6m$

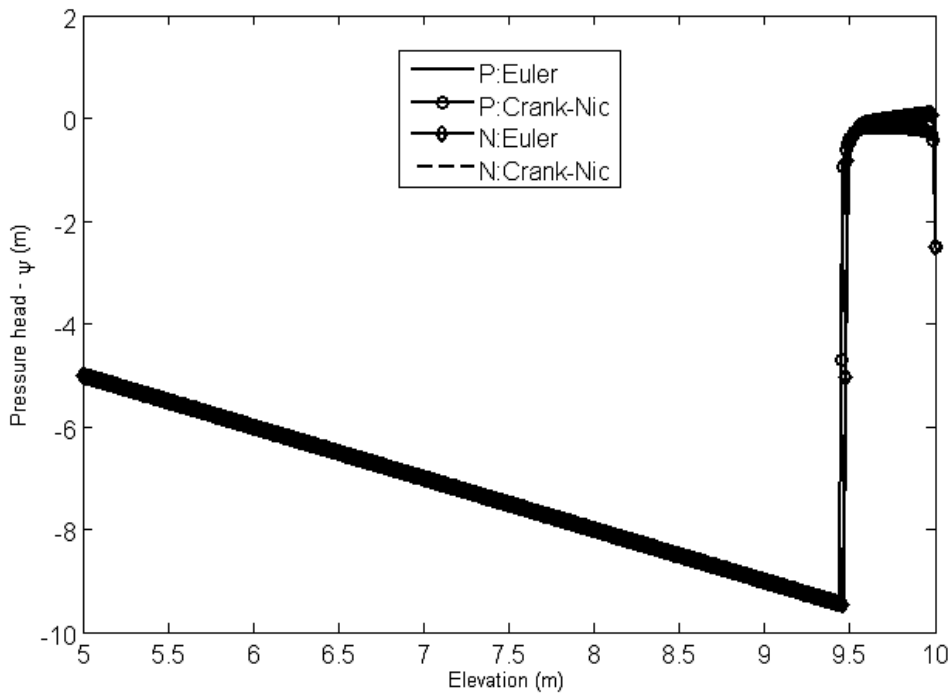

FIGURE 7. Pressure head profiles at time *0.325 days* for the Picard (Euler and Crank–Nicolson) and Newton (Euler and Crank–Nicolson) iterative schemes

and $1.2m$<z<$2m$ and Soil-II for $0.6m$<z<$1.2m$. A Dirichlet boundary condition is imposed at the base of the bottom boundary.

TABLE 5. Soil hydraulic properties used in Test case 5

Variables	Soil-I	Soil-II
θ_s (-)	0.35	0.35
θ_r (-)	0.07	0.035
α (cm^{-1})	0.0286	0.0667
n	1.5	3.0
K_s (cm/s)	9.81×10^{-5}	9.81×10^{-3}

FIGURE 9 shows the curves of simulated water saturation vs. elevation after 1050000s (approximately 12 days) time for implicit backward Euler and Crank–Nicolson methods, where the simulation is performed for a fine mesh of 150 elements. The simulated profiles in the

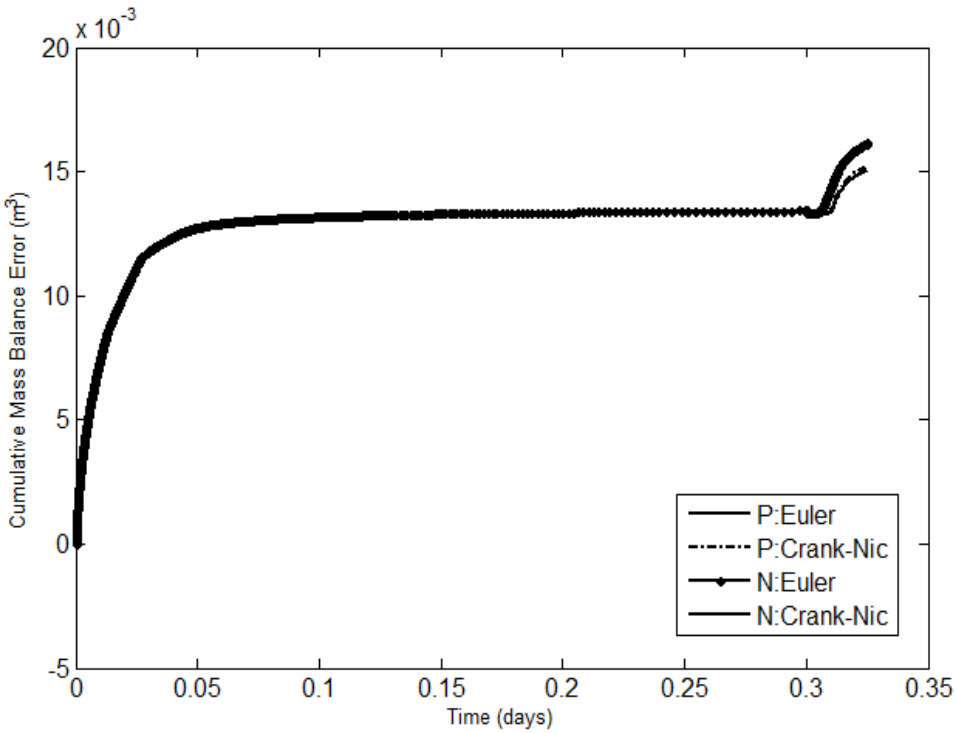

FIGURE 8. Evolution of mass balance errors for the entire simulation of Test case 4

Crank–Nicolson method are less efficient than those given by the backward Euler time discretization method for the first two layers, and both of them the fully implicit backward Euler method is considered as more reasonable. For the implicit backward Euler time discretization approach of Picard and Newton iterative schemes, the interesting characteristic of this simulation is that the middle medium sand layer tends to restrict drainage from the overlying fine sand and high saturation levels are maintained in the upper fine soil for a considerable period of time. Reduced drainage in the layered soil occurs because desaturation of the medium sand results in a very low relative permeability for this layer. This example illustrates the effectiveness of coarser-grained layers as capillary barriers in unsaturated flow. FIGURE 10 shows the mass balance errors for the implicit backward Euler approximation and the simulated statistics are listed in TABLE 6.

6. CONCLUSIONS

A finite element method has been developed and experimentally investigated for solving the Richards' equation using backward Euler and Crank–Nicolson time differencing schemes. This method is based on the Picard and Newton iterative formulation of the model equations,

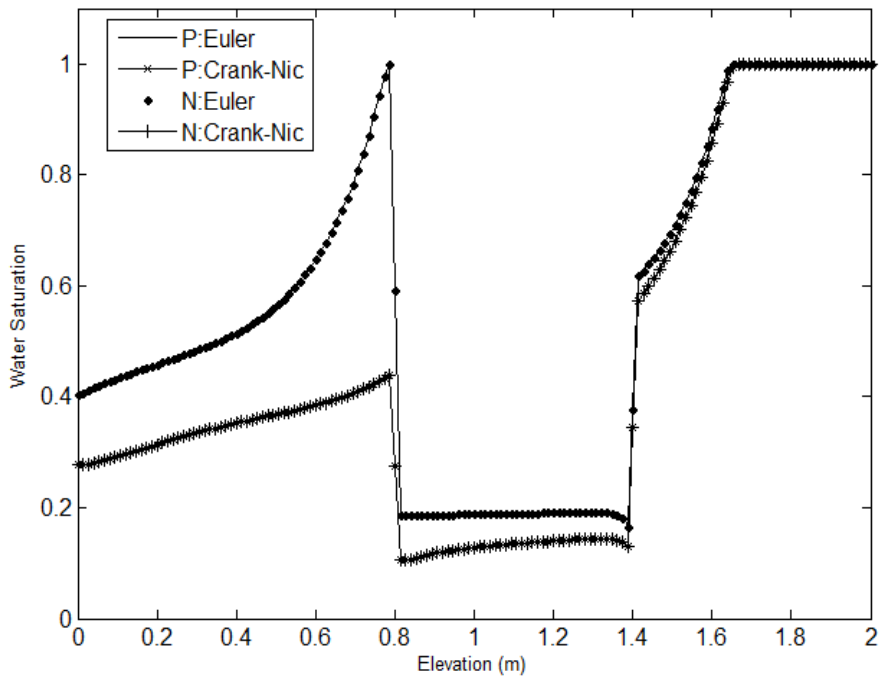

FIGURE 9. Saturation prediction after 12 days (approximately) for the Picard (Euler and Crank–Nicolson) and Newton (Euler and Crank–Nicolson) iterative schemes

TABLE 6. Summary statistics of the Test case 5

	Picard		Newton	
	Euler	Crank–Nicolson	Euler	Crank–Nicolson
MBE (m^3)	-6.589e-5	7.997e-3	9.601e-5	7.866e-3
MBE (%)	5.282e-1	-3.756e+2	-7.786e-1	-4.146e+2
No. of Time Steps	1147	1140	46165	100059
NL/Time steps	1.61	1.53	3.61	3.63

and is suitable for the simulation of variably saturated flow on homogeneous but not for heterogeneous soils. Since the finite element equations for this simpler implementation would involve lower order derivatives of the characteristic equations, errors arising in near-saturated regions would be reduced. Besides, pressure-head based form of Richards' equation for the work reported here was to maintain a consistent formulation for the two iterative strategies and dynamic time stepping can be easily handled. The numerical results presented exhibit clearly

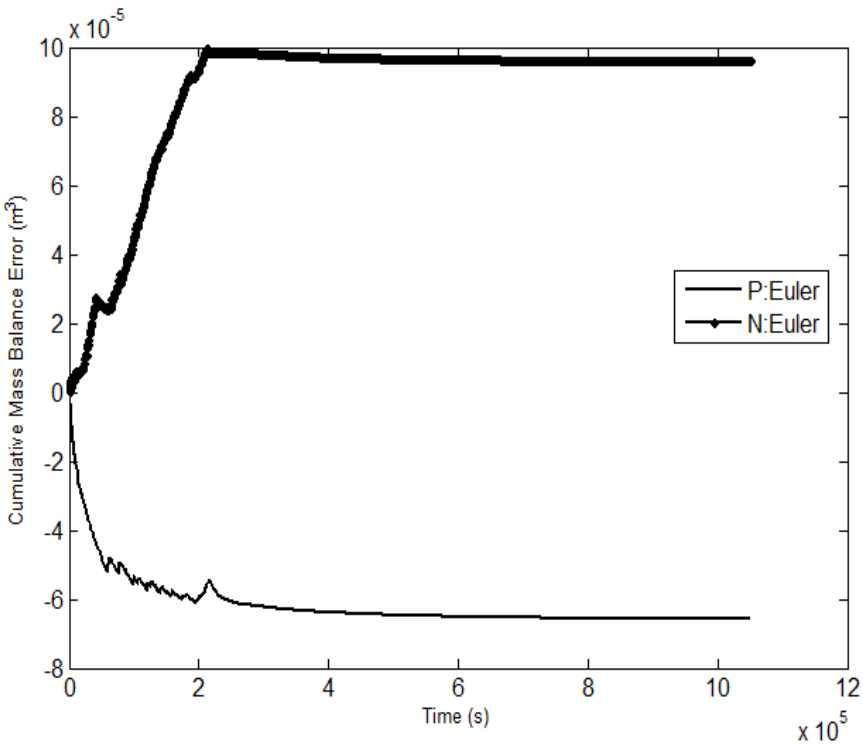

FIGURE 10. Evolution of mass balance errors for the entire simulation of Test case 5 for Euler method of Picard and Newton iterative schemes

that the formulation is effective in handling severely nonlinear cases of variably-saturated flow. The performance of the proposed scheme was evaluated by conducting five test simulations. For each of the tested homogeneous soil problems, the numerical results obtained from the two solution algorithms were almost identical, provided that the same spatial and temporal discretizations were employed. As well as, the results are in good agreement with the previous numerical studies and poses excellent mass balance property over the entire spatial mesh. For the layered soil test case, the Crank–Nicolson scheme incurred numerical instability or divergence under the same simulation conditions. The success of the algorithm in simulating a variety of problems leads to confidence in its applicability to many variably saturated/unsaturated multi-dimensional flow problems.

REFERENCES

[1] R. Jiwari: *A hybrid numerical scheme for the numerical solution of the Burgers' equation*, Computer Physics Communications, **188** (2015), 59-67.

[2] A. Verma, R. Jiwari and S. Kumar: *A numerical scheme based on differential quadrature method for numerical simulation of nonlinear Klein-Gordon equation*, International Journal of Numerical Methods for Heat & Fluid Flow, **24(2.6)** (2014), 1390-1404.

[3] R. Jiwari, S. Pandit and R. C. Mittal: *A Differential Quadrature Algorithm to Solve the Two Dimensional Linear Hyperbolic Telegraph Equation with Diriclet and Neumann Boundary Conditions,* Applied Mathematics and Computation, **218** (2012), 7279-7294.

[4] S. Pandit, M. Kumar and S. Tiwari: *Numerical simulation of second-order hyperbolic telegraph type equations with variable coefficients*, Computer Physics Communications, **187**(2015), 83-90.

[5] D. Sharma, R. Jiwari and S. Kumar: *A comparative study of Modal matrix and finite elements methods for two point boundary value problems*, Int. J. of Appl. Math. and Mech., **8(3.4)** (2012), 29-45.

[6] D. Sharma, R. Jiwari and S. Kumar:*Numerical solutions of two point boundary value problems using Galerkin-Finite element method*, Int. J. of Nonlinear Sciences, **13(2.1)**(2012), 204-210.

[7] S. Shukla, M. Tamsir and V. K. Srivastava: *Numerical simulation of two-dimensional sine-Gordon solitons by differential quadrature method*, Computer Physics Communications, **183** (2012), 600-616.

[8] B. Brunone, M. Ferrante, N. Romano and A. Santini: *Numerical simulations of one-dimensional infiltration into layered soils with the Richards' equation using different estimates of the interlayer conductivity,* Vadose Zone Journal, **2**(2003), 193–200.

[9] M. Celia, E. Bouloutas and R. Zarba: *A general mass-conservative numerical solution for the unsaturated flow equation,* Water Resour. Res., **26**(1990), 1483–1496.

[10] V. Lima-Vivancos and V. Voller: *Two numerical methods for modeling variably saturated flow in layered media,* Vadose Zone Journal **3**(2004), 1031–1037.

[11] J. Simunek, M. Sejna, H. Saito, M. Sakai and M. T. van Genuchten: *The HYDRUS-1D software pack-age for simulating the one-dimensional movement of water, heat and multiple solutes in variably-saturated media,* Version 4.0. Department of Environmental Sciences, University of California Riverside, Riverside, California. 2008.

[12] J. van Dam and R. Feddes: *Numerical simulation of infiltration, evaporation and shallow groundwater levels with the Richards' equation,* Journal of Hydrology, *233*(2000), 72–85.

[13] B. Belfort and F. Lehmann: *Comparison of equivalent conductivities for numerical simulation of one-dimensional unsaturated flow,* Vadose Zone Journal, **4**(2005), 1191–1200.

[14] H. Li, M. Farthing and C. Miller: *Adaptive local discontinuous Galerkin approximation to Richards' equation,* Adv. Water Resour., **30**(2007), 1883–1901.

[15] R. L. Cooley: *Some new procedures for numerical solution of variably saturated flow problems,* Water Resour. Res., **19**(1983), 1271-1285.

[16] E. O. Frind and M. J. Verge: Three-dimensional modeling of groundwater flow systems, Water Resour. Res., **14(2.4)**(1978), 844-856.

[17] R. G. Hills, I. Porro, D. B. Hudson and P. J. Wierenga: *Modeling of one dimensional infiltration into very dry soils: 1. Model development and evaluation,* Water Resour. Res., **25**(1989), 1259–1269.

[18] P. S. Huyakorn, S. D. Thomas and B. M. Thompson: *Techniques for making finite elements competitive in modeling flow in variably saturated media,* Water Resour. Res., **20**(1984), 1099-1115.

[19] P. S. Huyakorn, E. P. Springer, V. Guvanasen and T. D. Wadsworth: *A three dimensional finite element model for simulating water flow in variably saturated porous media,* Water Resour. Res., **22**(1986), 1790-1808.

[20] S. P. Neuman: *Saturated-unsaturated seepage by finite elements,* J. Hydraul. Div. ASCE, **99**(HY12)(1973), 2233-2250.

[21] P. Ross: *Efficient numerical methods for infiltration using Richards' equation,* Water Resour. Res., **26**(1990), 279-290.

[22] F. Lehmann and P. H. Ackerer: *Comparison of iterative methods for improved solutions of the fluid flow equation in partially saturated porous media,* Transport in Porous Media, **31**(1998), 275–292.

[23] C. Paniconi and M. Putti: *A comparison of Picard and Newton iteration in the numerical solution of multidimensional variably saturated flow problems,* Water Resour. Res., **30**(1994), 3357–3374.

[24] L. Bergamaschi and M. Putti: *Mixed finite elements and Newton-type linearizations for the solution for the unsaturated flow equation,* Int. J. Numer. Meth. Eng., **45**(1999), 1025–1046.

[25] C. Fassino and G. Manzini: *Fast-secant algorithms for the non-linear Richards Equation.* Communications in Numerical Methods in Engineering, **14**(1998), 921-930.

[26] D. Kavetski, P. Binning and S. W. Sloan: *Noniterative time stepping schemes with adaptive truncation error control for the solution of Richards' equation,* Water Resour. Res., **24**(2002), 595–605.

[27] A. A. Aldama and C. Paniconi: *An analysis of the convergence of Picard iterations for implicit approximations of Richards' equation,* in Proceedings of the IX International Conference on Computational Methods in Water Resources, edited by T. F. Russell, R. E. Ewing, C. A. Brebbia, W. G. Gray, and G. F. Pinder, pp. 521-528, Computational Mechanics Publications, Billedca, Mass., 1992.

[28] W. Brutsaer: *A functional iteration technique for solving the Richards' equation applied to two-dimensional infiltration problems,* Water Resour. Res., **7(2.5)**(1971), 1583-1596.

[29] C. R. Faust: *Transport of immiscible fluids within and below the unsaturated zone: A numerical model,* Water Resour. Res., **21(2.3)**(1985), 587-596.

[30] C. Paniconi, A. A. Aldama and E. F. Wood: *Numerical evaluation of iterative and noniterative methods for the solution of the nonlinear Richards equation,* Water Resour. Res., **27**(1991), 1147-1163.

[31] R. H. Brooks and A. T. Corey: *Hydraulic properties of porous media,* Hydrology Paper No.3, Civil Engineering, Colorado State University, Fort Collins, CO, 1964.

[32] M. T. van Genuchten: *A Closed-form Equation for Predicting the Hydraulic Conductivity of Unsaturated Soils,* Soil Sci. Soc. Am. J., **44(**1980), 892–898.

[33] C. T. Miller, G. A. Williams, C. T. Kelley, and M. D. Tocci: *Robust solution of Richards' equation for non uniform porous media,* Water Resour. Res., **34**(1998), 2599-2610.

[34] D. Kavetski, P. Binning and S. W. Sloan: *Adaptive backward Euler time stepping with truncation error control for numerical modelling of unsaturated fluid flow,* Int. J. Numer. Meth. Eng., **53**(2001a), 1301-1322.

[35] C. M. F. D'Haese, M. Putti, C. Paniconi and N. E. C. Verhoest: *Assessment of adaptive and heuristic time stepping for variably saturated flow*, Int. J. Numer. Meth. Fluids, **53**(2007), 1173–1193.

[36] V. Casulli and P. Zanolli: *A Nested Newton-type algorithm for finite volume methods solving Richards' equation in mixed form,* SIAM J. Sci. Comput., **32**(2010), 2255-2273.

[37] M. S. Islam and M. K. Hasan (2014): *An application of nested Newton-type algorithm for finite difference method solving Richards' equation,* IOSR Journal of Mathematics, **10**(2014), 20-32.

[38] K. Rathfelder and L. M. Abriola: *Mass conservative numerical solutions of the head-based Richards' equation,* Water Resour. Res., **30(9)**(1994), 2579-2586.

[39] M. D. Tocci, C. T. Kelley, and C. T. Miller: *Accurate and economical solution of the pressure-head form of Richards' equation by the method of lines*, Adv. Water Resour., **20(1)**(1997), 1-14.

[40] C. T. Miller, C. Abhishek and M. Farthing: *A spatially and temporally adaptive solution of Richards' equation,* Adv. Water Resour., **29**(2006), 525–545, 2006.

[41] M. S. Islam and M. K. Hasan: *Accurate and economical solution of Richards' equation by the method of lines and comparison of the computational performance of ODE solvers,* International Journal of Mathematics and Computer Research, **2**(2013), 328-346.

[42] C. E. Kees and C. T. Miller: *Higher order time integration methods for two-phase flow,* Adv. Water Resour., **25(2.1)**(2002), 159–77.

[43] M. S. Islam and M. K. Hasan: *An investigation of temporal adaptive solution of Richards' equation for sharp front problems,* IOSR Journal of Mathematics, **10(2.1)**(2014), 106-117.

[44] D. McBride, M. Cross, N. Croft, C. Bennett and J. Gebhardt: *Computational modeling of variably saturated flow in porous media with complex three-dimensional geometries,* Int. J. Numer. Meth. Fluids, **50**(2006), 1085–1117.

[45] F. Marinelli and D. S. Durnford: *Semi analytical solution to Richards' equation for layered porous media,* J. Irrigation Drainage Eng., **124**(1998), 290–299.